

Observation of a continuous phase transition in a shape-memory alloy

J. C. Lashley,¹ S. M. Shapiro,² B. L. Winn,³ C. P. Opeil,⁴ M. E. Manley,⁵ A. Alatas,⁶ W. Ratcliff,⁷
T. Park,^{1,8} R. A. Fisher,¹ B. Mihaila,¹ P. Riseborough,⁹ E. K. H. Salje,¹⁰ and J. L. Smith¹

¹*Los Alamos National Laboratory, Los Alamos, NM 87545, USA*

²*Brookhaven National Laboratory, Upton, NY 11973, USA*

³*Oak Ridge National Laboratory, Oak Ridge, TN 37831, USA*

⁴*Boston College, Department of Physics, 140 Commonwealth Avenue, Chestnut Hill, MA 02467, USA*

⁵*Lawrence Livermore National Laboratory, Livermore, CA 94550, USA*

⁶*Advanced Photon Source, Argonne National Laboratory, Argonne, IL 60439, USA*

⁷*National Institute of Standards and Technology, Gaithersburg, MD 20899, USA*

⁸*Department of Physics, Sungkyunkwan University, Suwon 440-746, Korea*

⁹*Department of Physics, Temple University, Philadelphia, PA 19122, USA*

¹⁰*Department of Earth Sciences, University of Cambridge, Downing Street, Cambridge CB2 3EQ, UK*

Elastic neutron-scattering, inelastic x-ray scattering, specific-heat, and pressure-dependent electrical transport measurements have been made on single crystals of AuZn and Au_{0.52}Zn_{0.48} above and below their martensitic transition temperatures ($T_M = 64$ K and 45 K, respectively). In each composition, elastic neutron scattering detects new commensurate Bragg peaks (modulation) appearing at $Q = (1.33, 0.67, 0)$ at temperatures corresponding to each sample's T_M . Although the new Bragg peaks appear in a discontinuous manner in the Au_{0.52}Zn_{0.48} sample, they appear in a continuous manner in AuZn. Surprising us, the temperature dependence of the AuZn Bragg peak intensity and the specific-heat jump near the transition temperature are in favorable accord with a mean-field approximation. A Landau-theory-based fit to the pressure dependence of the transition temperature suggests the presence of a critical endpoint in the AuZn phase diagram located at $T_M^* = 2.7$ K and $p^* = 3.1$ GPa, with a quantum saturation temperature $\theta_s = 48.3 \pm 3.7$ K.

PACS numbers: 81.30.Kf, 71.20.Be,

A class of materials exhibiting martensitic (diffusionless) phase transformations yields properties used in a range of technological applications including implants to increase flow in restricted blood vessels [1], actuators for the treatment of high myopia [2], voltage generators [3], and orthodontic arch-wires [4]. These properties often depend on the history of the material and may allow it to recover its previous shape after deformation, known as the shape-memory effect (SME). It has long been recognized that these transformations are all thermodynamically first order (discontinuous) [5, 6, 7]. Special cases arise when the order parameter is coupled to an external field in a complicated way, leading to a weakly first-order transition [8], which is believed to result from a complicated coupling between strain and order parameter fluctuations. Because shape-memory alloys and other multiferroic materials owe their functionality to complicated cross-field responses between two (or more) pairs of conjugate thermodynamic variables, a description of the free-energy landscape and the ability to predict functionality become one and the same.

Phenomenological descriptions of the martensitic transformation pathway, based on reciprocal space [9] and real space [10] geometries, have established rules to determine relative twin and crystallographic orientations between the austenite (high-temperature) and martensite (low-temperature) modifications. Knowledge of the symmetry breaking allows for a definition of the energetic driving force in terms of the difference in free energies be-

tween phases. In the Ginzburg-Landau (GL) approach, the free energy, G , is expressed as a sum of symmetry invariants. In its simplest form, G is approximated by a polynomial expansion in even powers of an order parameter, Q , as $G(Q) = aQ^2 + bQ^4 + cQ^6 + \frac{g}{2}|\nabla Q|^2$. For martensitic transformations, Q is taken to be strain or strain coupled to shuffle (displacements involving quasi-static phonons with fractional commensurate wave vectors with uniform shears [11]). The coefficients a, b, c , and g are material parameters to be determined experimentally or by first principle simulations.

For the majority of shear-induced transformations, the GL expansion captures the essential physics [12, 13], such as constitutive response [14, 15] and the occurrence of anti-phase boundaries [16]. When applied to shape-memory alloys, the presence of intervening (premartensitic) phases [17] presents difficulties for both experiment and theory as to a unique characterization of the order parameter. Further issues have arisen in materials exhibiting quantum mechanical effects in the band structure and strong electron-phonon coupling [18]. The thermodynamic behavior is best explored when no further transitions occur between T_M and 0 K. This effect was recently reported for Fe-doped NiTi, where all thermodynamic parameters could be correlated self-consistently within mean field theory [19]. In order to integrate these cases into GL theory, it is necessary to measure and access each thermodynamic property and infer cross-field couplings of the order parameter. The ability to distin-

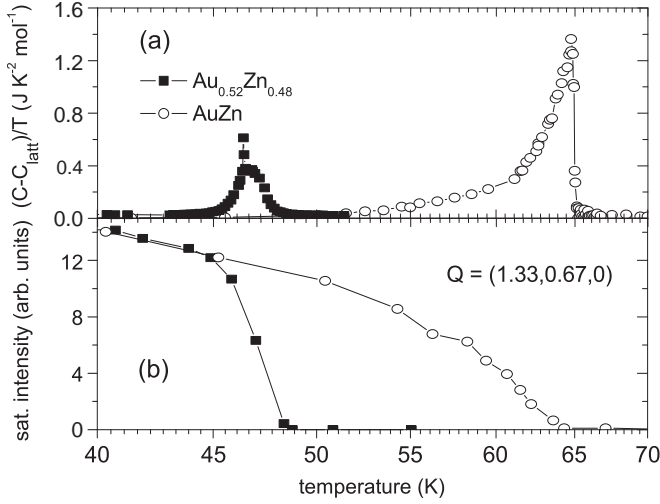


FIG. 1: (a) The excess specific heat divided by temperature versus temperature in the vicinity of the martensitic transitions for $\text{Au}_{0.52}\text{Zn}_{0.48}$ and AuZn . (b) Temperature dependence of the satellite-peak intensity along $Q = (1.33, 0.67, 0)$. The satellite peak intensity is proportional to the square of the order parameter.

guish subtle differences between first-order and weakly first-order depends on the ability to resolve the behavior of pertinent physical properties.

In this Letter we examine the AuZn system for thermodynamic properties that contribute to the first-order or weakly first-order nature of the free-energy landscape. We measure elastic neutron-scattering, inelastic x-ray scattering, specific-heat, and the pressure dependence of the transition by electrical transport. While we observed classical first-order behavior at 45 K for $\text{Au}_{0.52}\text{Zn}_{0.48}$, we observed a mean field continuous transformation for AuZn near 64 K in the temperature dependence of the Bragg peak intensity, and a Landau step with a λ anomaly in the excess specific heat.

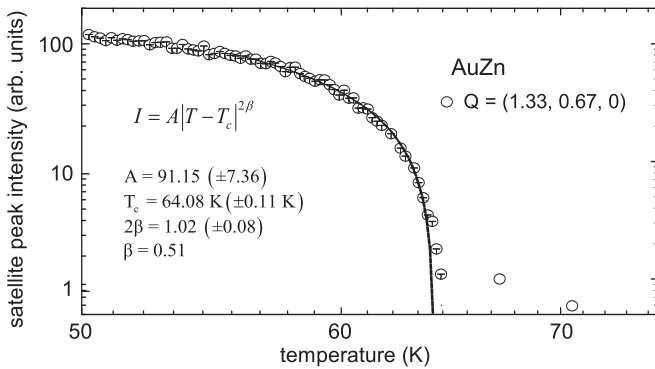


FIG. 2: Temperature dependence of the satellite peak intensity on heating along $Q = (1.33, 0.67, 0)$ in AuZn , near the transition temperature. A fit to mean-field theory for $T \leq T_c$. The points above 64 K are background.

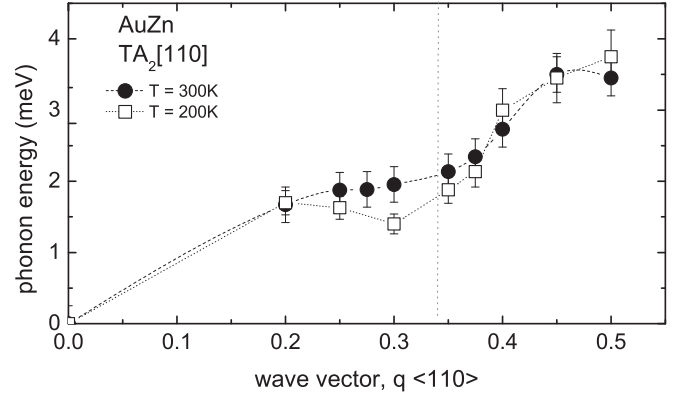


FIG. 3: Temperature dependence of the phonon dispersion in AuZn along the TA_2 branch. At 300 K one notices considerable phonon softening at $q = (0.33, 0.33, 0)$ (vertical line). The dashed lines between points are provided as guides to the eye.

Single crystals were prepared by fusion of the elements in a Bridgman furnace and were oriented by back-reflection Laue diffraction. The neutron experiments were performed on the BT9 triple-axis spectrometer at the NIST research reactor. Measurements of the phonon dispersion were made on XOR of sector 3 at the Advanced Photon Source, Argonne National Laboratory [20, 21]. Specific-heat measurements were measured using a thermal-relaxation calorimeter by Quantum Design [22]. The pressure dependence of the transition temperature was made by a four-terminal ac-transport method in a mechanical pressure cell designed to reach pressures of 3 GPa.

Previous investigations have shown that AuZn exhibits a martensitic transition as seen with low-temperature electron microscopy [23] and by recoverable transformation strain (shape-memory effect) [24]. Figure 1 shows the temperature dependence of (a) the excess specific heat and (b) the satellite peak intensity for $\text{Au}_{0.52}\text{Zn}_{0.48}$ and AuZn . Although we have measured the specific heat previously [25], it is plotted along with the elastic neutron-scattering data, since it is revealing to compare both sets of measurements that were made on the same samples. We find a latent heat anomaly at 45 K for $\text{Au}_{0.52}\text{Zn}_{0.48}$. A λ -anomaly was observed for AuZn , but no latent heat was observed. The specific heat near the transition can be influenced by intrinsic defects, including triple-point and anti-structure defects, both known to be present in the B2 structure [26, 27]. It was therefore necessary to use a microscopic probe to determine whether or not the transition could be a broadened first-order transition. Elastic neutron-scattering measurements indicate that in each composition new commensurate Bragg peaks (modulation) appear at $Q = (1.33, 0.67, 0)$ at temperatures corresponding to each sample's T_M Figure 1(b). Mirroring the specific-heat data, the temperature depen-

dence of the satellite peak intensity shows a rapid jump at 45 K in $\text{Au}_{0.52}\text{Zn}_{0.48}$, while a continuous variation occurs for AuZn on warming starting at 64 K. The satellite peak intensity is proportional to the square of the order parameter, since it leads to the low-temperature rhombohedral phase. The specific-heat data also indicate thermal hysteresis (not shown) of 6 K at 45 K for $\text{Au}_{0.52}\text{Zn}_{0.48}$. The satellite peak intensity for AuZn depicted in Fig. 1(b) was measured by neutrons on heating and cooling. Unlike the specific-heat data Fig. 1(a) we observe a small discontinuity and 1.5 K difference in transition temperature on cooling.

Figure 2 shows the satellite peak intensity versus temperature in the vicinity of T_M for AuZn. Near the transition temperature, the satellite peak evolves continuously with increasing temperature, showing a temperature dependence given by $I = A|T - T_M|^{2\beta}$; where the satellite peak intensity is I , the critical temperature is T_M , and the critical exponent is β . We obtain $T_M = 64.08 \text{ K} \pm 0.11 \text{ K}$ and $2\beta = 1.02 \pm 0.08$. The value of the critical exponent obtained from this fit ($\beta = 0.51$) is close to the mean-field value of $\beta = 0.50$ [28]. One could argue that mean-field exponents were obtained by coincidence given that the critical regime, as defined by the Ginzburg-criterion, is restricted to a range of temperatures too small to be resolved by our experiments, or that the correlation length does not diverge, since it is limited by other extrinsic disorder (*i.e.*, martensite twins) or intrinsic fluctuations. The latter possibility seems more

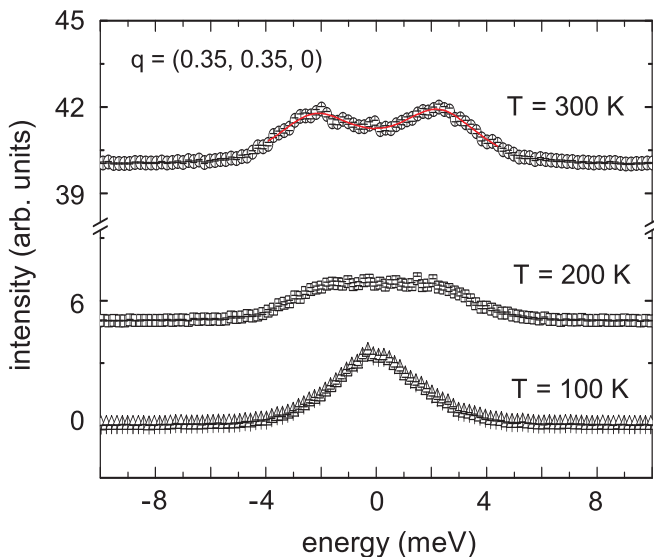


FIG. 4: Inelastic x-ray scattering data showing the temperature dependence near the soft mode, $q = (0.35, 0.35, 0)$. The 300 and 200 K data are offset by 0.004 and 0.0005, respectively on the y-axis for clarity. The energy positions are fit to a double Lorentzian (solid curve) at 300 K to determine the phonon energy. The intrinsic resolution for inelastic x-ray scattering is 2 meV.

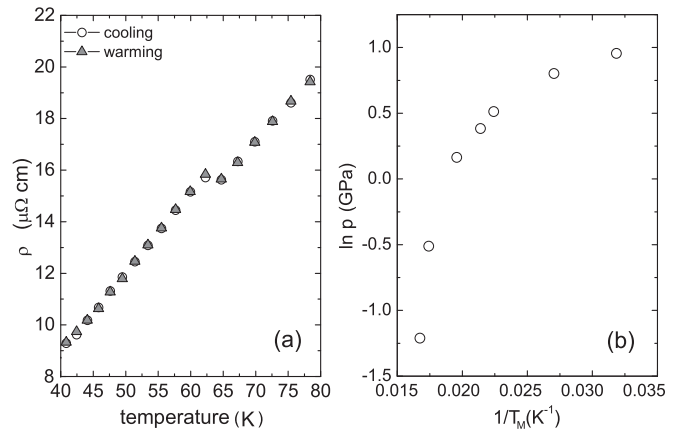


FIG. 5: (a) The electrical-resistivity data taken on cooling and warming is shown in the vicinity of T_M . (b) Plot of $\ln p$ versus $1/T$ to test the applicability Clausius-Clapeyron equation.

plausible to us, because the inverse correlation length, or width of the Bragg peaks (not shown), increases as the temperature is lowered below T_M .

As the temperature is lowered, the unit cell is modulated in the [110] shear direction. A commensurate shuffle of every third unit cell results in a hexagonal primitive unit cell formed from nine primitive cubic cells of the parent phase. This structure can also be described in terms of its conventional rhombohedral unit cell. In Fig. 3 we show the TA_2 phonon-dispersion curves along [110], measured by inelastic x-ray scattering at temperatures of 300 K and 200 K. The inflection in the phonon frequency near $\xi = 1/3$ indicates the low shear instability along the TA_2 [110] branch. This inflection is comparable to an earlier investigation [29] of off-stoichiometric AuZn samples. At 300 K, the phonon energy positions have been fit over the energy range $-4 \text{ meV} \leq E \leq 4 \text{ meV}$ to a double Lorentzian, as shown in Figure 4. The phonons continuously soften with decreasing temperature to the point where separation becomes difficult below 200 K.

Figure 5 (a) shows the change in resistivity between cooling and warming. The data were collected with warming and cooling rates of 0.2 K min^{-1} . In the region of T_M there is no hysteresis, to within experimental error. Because of the lack of hysteresis, we elected to measure the pressure dependence of the transition. For a first-order transition, the Clausius-Clapeyron relation, $\ln p/p_0 = -\Delta H/(RT) + A$, predicts a linear relationship for $\ln p/p_0$ versus $1/T$ with the slope $(-\Delta H/R)$. Here, p denotes the pressure, H the enthalpy, R the universal gas constant, and p_0 is a reference pressure. Figure 5(b) shows the plot of $\ln p$ versus $1/T$. It appears that there is no observable linear region. Assuming that the entropy does not vary significantly with pressure, the conditions for the applicability of the Clausius-Clapeyron relation are not met. This result provides further evidence that

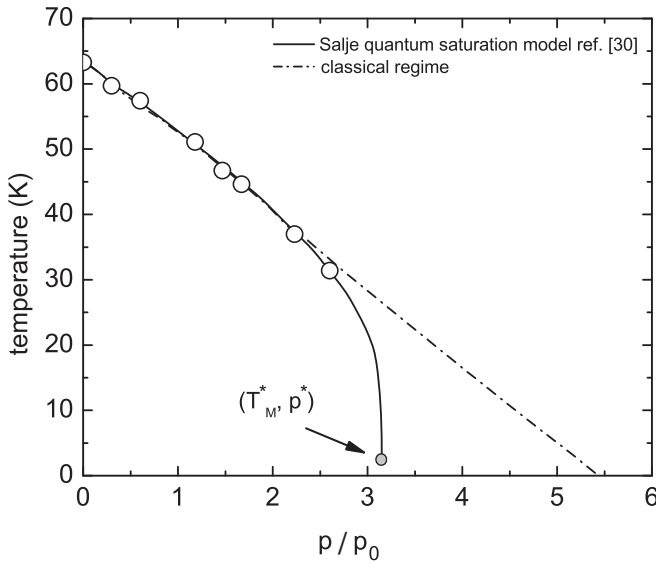


FIG. 6: Pressure dependence of the transition temperature up to pressures of nearly 3 GPa, together with a fit to Salje's model [30] which accounts for quantum saturation effects close to zero absolute temperature. The difference between the linear (classical) and quantum-dominant behavior is illustrated in the inset. We find that quantum effects become important for temperatures lower than $\theta_s = 48.3 \pm 3.7$ K, and a critical endpoint is predicted at $T_M^* = 2.7$ K and $p^* = 3.1$ GPa.

the transition is not first order.

We use a modified GL free energy expression to describe the quantum saturation in the order parameter expected at sufficiently low temperature [30]. This saturation effect reflects the departure from classical behavior as the absolute temperature approaches zero and is a direct consequence of the third law of thermodynamics. Following Salje *et al.* [30], we fit the pressure dependence of the transition as $\theta_s/T_M(p) = \coth^{-1}[\coth(\theta_s/T_M(0)) - p/p_0]$. Here θ_s is a phenomenological temperature below which quantum mechanical effects are dominant. We find $p_0 = 5.6 \pm 0.7$ GPa and $\theta_s = 48.3 \pm 3.7$ K. The resulting phase diagram predicts a critical endpoint at $T_M^* = 2.7$ K and $p^* = 3.1$ GPa. Figure 6 depicts the experimental pressure dependence of the transition temperature for pressures up to nearly 3 GPa, together with the fit to Salje's classical regime. We find a classical slope of -11.7 ± 0.2 K GPa $^{-1}$. The difference between the classical and quantum regimes is important for temperatures below θ_s .

In conclusion, we report results of a detailed experimental study of the martensitic transition in AuZn. While the temperature dependence of the satellite peak intensity (proportional to the square of the order parameter) show marked first-order behavior at 45 K for Au_{0.52}Zn_{0.48}, we observed a continuous feature well-described by a mean-field exponent ($\beta=0.51$) for AuZn at 64 K. This result is contrary to the established def-

inition of a martensitic transition. Providing supporting evidence to the continuous nature of the phase transition in AuZn are the lack of thermal hysteresis from electrical-resistivity measurements, the λ -anomaly in the specific heat, and the disagreement of pressure data with the Clausius-Clapeyron relation. Using Salje's model to describe the quantum saturation effects close to zero absolute temperature, we predict the presence of a critical endpoint in the phase diagram located at $T_M^* = 2.7$ K and $p^* = 3.1$ GPa, with a phenomenological temperature $\theta_s = 48.3 \pm 3.7$ K for the onset of quantum effects.

This work was performed under the auspices of the United States Department of Energy and Department of Commerce and supported in part by the Trustees of Boston College. Work at Brookhaven is supported by the Office of Science, United States Department of Energy under Contract No. DE-ACO2-98CH10886. The use of the Advanced Photon Source was supported by the U.S. Department of Energy, Office of Science, Office of Basic Energy Sciences, under Contract No. DE-AC02-06CH11357.

-
- [1] P. W. Duerig, MRS Bulletin **27**, 101 (2002).
 - [2] I. Yu *et al.*, Mater. Sci. Eng. A **481-482**, 651 (2008).
 - [3] I. Suorsa *et al.*, J. Appl. Phys. **95**, 8054 (2004).
 - [4] J. Jafari, S. M. Zebajad, and S. A. Sajjadi, Mater. Sci. Eng. A. **473**, 42 (2008).
 - [5] R. C. Albers *et al.*, Comp. and Appl. Math. **23**, 345 (2004).
 - [6] J. G. Boyd and D. C. Lagoudas, Int. J. Plasticity **12**, 805 (1996).
 - [7] P. W. Gash, J. Appl. Phys. **54**, 6900 (1983).
 - [8] S. Rubini and P. Ballone, Phys. Rev. B. **48**, 99, (1993).
 - [9] J. S. Bowles and J. K. Mackenzie, Act. Met. **2**, 129 (1954).
 - [10] M. S. Wechsler, D. S. Lieberman, and T. A. Read, J. of Metals **5**, 1503 (1953).
 - [11] W.G. Burgers, Physica Utrecht **1**, 561 (1934).
 - [12] P. Toledano and P. Toledano, The Landau Theory of Phase Transformations (World Scientific, Singapore, 1987).
 - [13] E. K. H. Salje, Phase Transformations in Ferrelastic and Co-elastic Solids (Cambridge University Press, Cambridge, UK, 1990).
 - [14] R. Ahluwalia *et al.*, Acta. Mat. **52**, 209 (2004).
 - [15] M. Iwata and Y. Ishibashi, J. Phys. Soc. Jap. **72**, 2843 (2003).
 - [16] W. Cao, A. Saxena, and D. M. Hatch, Phys. Rev. B. **64**, 024106 (2001).
 - [17] S. Kartha *et al.*, Phys. Rev. Lett. **67**, 3630 (1991).
 - [18] K. H. Ahn *et al.*, Phys. Rev. B. **71**, 212102 (2005).
 - [19] E. K. H. Salje *et al.*, J. Phys. Cond. Matt., **20**, 275216 (2008).
 - [20] H. Sinn *et al.*, Nucl. Inst. and Meth. in Phys. Res. A **467**, 1545 (2001).
 - [21] H. Sinn, J. Phys. Cond. Matter **13**, 7525 (2001).
 - [22] J. C. Lashley *et al.*, Cryogenics **43**, 369 (2003).

- [23] H. Pops and T. B. Massalski, Trans. Met. Soc. AIME **223**, 728 (1965).
- [24] T. Darling *et al.*, Phil. Mag. B. **82**, 825 (2002).
- [25] R. McDonald *et al.*, J. Phys. Cond. Mat. **17**, L69 (2005).
- [26] Y. A. Chang and J. P. Neumann, Prog. Sol. St. Chem. **14**, 221 (1985).
- [27] D. Gupta and D. S. Lieberman, Phys. Rev. B. **4**, 1070 (1971).
- [28] J. J. Binney, N. J. Dowrick, A. J. Fisher, and M. E. J. Newman, Theory of Critical Phenomena (Oxford Science Publications, Oxford University Press Inc., New York, 1993).
- [29] T. Makita *et al.*, Phys. B. **213**, 430 (1995).
- [30] S. A. Hayward and E. K. H. Salje, J. Phys.: Condens. Matter **10**, 1421 (1998); J. M. Pérez-Mato and E. K. H. Salje, *ibid.* **12**, L29 (2000).